

One-directional thermal transport in densely aligned single-wall carbon nanotube films

Cite as: Appl. Phys. Lett. **115**, 223104 (2019); doi: [10.1063/1.5127209](https://doi.org/10.1063/1.5127209)

Submitted: 10 September 2019 · Accepted: 7 November 2019 ·

Published Online: 27 November 2019







View Online



Export Citation



CrossMark

Shingi Yamaguchi,¹ Issei Tsunekawa,¹ Natsumi Komatsu,² Weilu Gao,²  Takuma Shiga,¹  Takashi Kodama,¹ Junichiro Kono,^{2,3,4,a)}  and Junichiro Shiomi^{1,b)} 

AFFILIATIONS

¹Department of Mechanical Engineering, The University of Tokyo, 7-3-1, Hongo, Bunkyo-ku, Tokyo 113-8656, Japan

²Department of Electrical and Computer Engineering, Rice University, Houston, Texas 77005, USA

³Department of Physics and Astronomy, Rice University, Houston, Texas 77005, USA

⁴Department of Materials Science and NanoEngineering, Rice University, Houston, Texas 77005, USA

^{a)}kono@rice.edu

^{b)}shiomi@photon.t.u-tokyo.ac.jp

ABSTRACT

Individual carbon nanotubes (CNTs) possess extremely high thermal conductivities. However, the thermal conductivities and their anisotropy of macroscopic assemblies of CNTs have so far remained small. Here, we report the results of directional thermal transport measurements on a nearly perfectly aligned CNT film fabricated via controlled vacuum filtration. We found the thermal conductivity to be $43 \pm 2.2 \text{ W m}^{-1} \text{ K}^{-1}$ with a record-high thermal anisotropy of 500. From the temperature dependence of the thermal conductivity and its agreement with the atomistic phonon transport calculation, we conclude that the effect of intertube thermal resistance on heat conduction in the alignment direction is negligible because of the large contact area between CNTs. These observations thus represent ideal unidirectional thermal transport, i.e., the thermal conductivity of the film is determined solely by that of individual CNTs.

Published under license by AIP Publishing. <https://doi.org/10.1063/1.5127209>

Thermal management in electronics is becoming more and more important as the degree of device miniaturization has reached a truly nanometer scale where the level of power dissipation is also extreme. Therefore, thermally conducting electronic nanomaterials are strongly required for more efficient heat dissipation. Carbon nanotubes (CNTs) are one of the most promising candidates, since individual CNTs have exhibited thermal conductivities (κ) over $10^3 \text{ W m}^{-1} \text{ K}^{-1}$.^{1–5} There have also been many thermal conductivity studies of CNT assemblies. In particular, κ has been measured for aligned CNT samples prepared by either direct chemical vapor deposition growth^{6–16} or postprocessing of synthesized CNTs, such as mechanical processing,^{17–22} direct spinning,²³ and magnetic alignment.^{24–26} However, the κ values reported for aligned CNT materials have so far been limited from tens to hundreds of watts per meter-Kelvin, significantly lower than those for individual CNTs. This drastic difference has been attributed to structural issues such as low volume fractions (0.5 ~ 50%), high defect densities, and low degrees of alignment, which make the intertube thermal resistance limit the film thermal conductivity. Therefore, it is essential to eliminate these structural deficiencies to utilize the high κ of individual CNTs in aligned CNT assemblies.

In addition to the general need for materials with high thermal conductivity, there is also a specific demand for materials with anisotropic thermal conductivity that can direct heat flow only in a certain direction. For example, when spreading the heat from a chip on a circuit board, such directional heat flow can prevent heat-sensitive components from being damaged by excess heat conducted from heat-generating parts.²⁷ CNTs are clearly good candidates because of their unique one-dimensional structure. However, unexpectedly, the thermal anisotropy of aligned CNT assemblies has not exceeded 100 in previous reports.^{6–9,16–20,24,25}

Here, we demonstrate a record-high value of thermal conductivity anisotropy in macroscopic films of aligned and packed CNTs prepared by the recently developed controlled vacuum filtration (CVF) method.^{28,29} Using the T-type and time-domain thermoreflectance (TDTR) methods, we obtained a thermal anisotropy of 500 at room temperature (RT), which is the largest value obtained among all previously studied macroscopic CNT assemblies.^{6–9,16–20,24,25} Although the κ in the alignment direction (κ_{\parallel}) is lower than the highest reported values,^{6–26} further theoretical analysis reveals that the κ_{\parallel} is determined only by the κ of the constituent CNTs and is not limited by intertube thermal resistance.

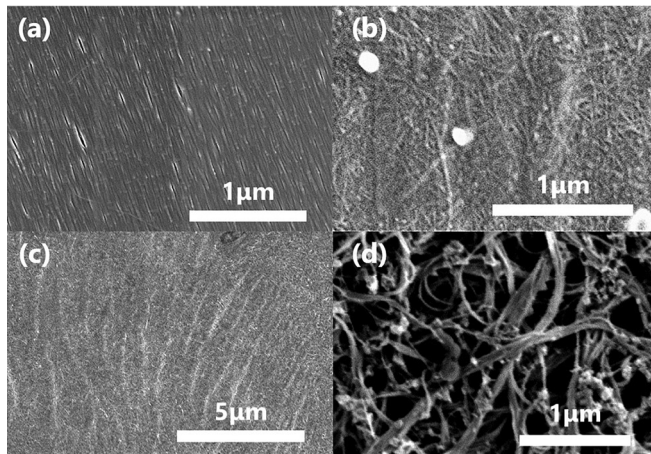


FIG. 1. Scanning electron microscopy (SEM) images: (a) Film 1 (highly aligned film prepared by the CVF method), (b) Film 2 (poorly aligned film prepared by the CVF method with NaCl addition), (c) Film 2 with lower magnification than (b) and (d) Film 3 (randomly aligned film prepared by filtration of a CNT dispersion without any additives or filtration control).

The CNT used in this study was unsorted arc-discharge CNT purchased from Carbon Solutions, Inc., and the highly aligned CNT films (Film 1) were prepared by the CVF method.²⁸ In addition, a poorly aligned CNT film (Film 2) and a randomly aligned CNT film (Film 3) were also prepared for comparison. Film 2 was prepared by filtrating the CNT dispersion with additional 6 mM of NaCl at a filtration speed four times higher than that in the case of Film 1. These changes alter the interaction between the CNTs and the filter membrane²⁸ and reduce the degree of alignment. Film 3 was prepared by filtration of a CNT dispersion without any additives or filtration control. κ_{\parallel} for each sample was measured by the T-type method^{1,30} (Fig. S1). The ~ 200 -nm-thick Films 1 and 2 were supported by the polyethylene terephthalate (PET) substrates, and their κ_{\parallel} values were calculated by subtracting the thermal conductance of the PET substrate from the thermal conductance of the CNT/PET (CNT and PET). Film 3 was ~ 30 μm thick and measured as a self-standing film. The cross-plane κ (κ_{\perp}) of Film 1 was measured using TDTR^{31,32} after coating the surface with an ~ 100 -nm-thick Al transducer film. The details of our TDTR setup are described elsewhere.³³

Top-view Scanning Electron Microscope (SEM) images of each sample are shown in Fig. 1. Film 1 [Fig. 1(a)] had uniformly aligned CNTs, as in previous reports.^{28,29,34–39} The alignment of Film 2 [Figs. 1(b) and 1(c)] is much weaker. The focused SEM image in Figs. 1(b) shows that the CNTs are oriented rather randomly, but there are parts with higher density due to the local moderate alignment that

gives rise to the different color contrast. This is more evident in the broad view [Fig. 1(c)] where white lines indicate partial ordering in Film 2. The morphology of Film 3 [Fig. 1(d)] was clearly different from that of the other two aligned samples; most CNTs existed as large bundles with a diameter of ~ 100 nm, and they formed a sparse network structure. The alignment degrees of Films 1 and 2 were evaluated by measuring the reduced linear dichroism (LD') with a 660 nm laser beam.³⁸ LD' was 0.68 for Film 1 and 0.040 for Film 2, and so the alignment degree of Film 2 was less than one tenth of that of Film 1 (Table I). The nonzero LD' value of Film 2 is also consistent with the ordering of CNTs seen in Fig. 1(c).

The κ measurements of the three films were conducted over a temperature range from 50 to 300 K. First, κ values of different samples at RT were compared to see any thermal property differences caused by the morphological differences and are summarized in Table I. The κ of Film 1 in the alignment direction ($\kappa_{\parallel,1} = 43 \pm 2.2$ $\text{W m}^{-1} \text{K}^{-1}$) at RT was higher than those of Film 2 ($\kappa_{\parallel,2} = 28 \pm 1.2$ $\text{W m}^{-1} \text{K}^{-1}$) and Film 3 ($\kappa_{\parallel,3} = 14 \pm 2.8$ $\text{W m}^{-1} \text{K}^{-1}$). On the other hand, the κ of Film 1 in the perpendicular direction ($\kappa_{\perp,1}$) was as low as 0.085 ± 0.017 $\text{W m}^{-1} \text{K}^{-1}$, which is three orders of magnitude smaller than $\kappa_{\parallel,1}$. This reveals that Film 1 had an extremely large thermal anisotropy ($\kappa_{\parallel,1}/\kappa_{\perp,1}$) of 500, which is the largest reported value among aligned CNT films.^{6–9,16–20,24,25} The highest and second-highest values of $\kappa_{\parallel,1}$ and $\kappa_{\parallel,2}$ show the κ_{\parallel} improvement of the film by the constituent CNT alignment, and the details of which will be discussed later. While the randomly aligned Film 3 showed lowest κ_{\parallel} , its structure seen in Fig. 1(d) contains seemingly aggregated CNT chunks. Therefore, it is difficult to separate the effect of aggregation from that of alignment. Therefore, the case of Film 3 is shown only to compare the absolute thermal conductivity value of conventional CNT mat with those of the aligned ones, and thus, the detailed heat conduction mechanism in Film 3 will not be discussed in this paper.

It is known that the κ values of CNT bundles are lower than those of individual CNTs due to the quenching of low-frequency phonon modes and small thermal conductance between CNTs.^{5,19,41,42} However, despite the nearly perfect CNT alignment in Film 1, its $\kappa_{\parallel,1}$ value at RT is still one order of magnitude smaller than the reported κ of a single CNT bundle ($\kappa_{\parallel,\text{bundle}}$).^{41–43} To understand the reason, the temperature dependence of $\kappa_{\parallel,1}$ was examined in detail. First, the temperature dependence of $\kappa_{\parallel,1}$ was compared with that of $\kappa_{\parallel,\text{bundle}}$ measured in Ref. 43. As shown in Fig. 2, the profiles normalized by the RT value show good agreement. In Ref. 43, CNT-CNT contact thermal resistance had negligible effects on $\kappa_{\parallel,\text{bundle}}$ because both the bundle itself and the constituent CNTs were 1 μm long; namely, all the CNTs seamlessly connected the two thermostats that suspended the bundle. Therefore, considering that the internal thermal conductance grows linearly with temperature⁴ and the intertube thermal conductance depends weakly on temperature^{40,43} in the range from 150 to 300 K,

TABLE I. LD' and κ at RT of the three films studied.

	Film 1 (highly aligned)	Film 2 (poorly aligned)	Film 3 (Randomly aligned)
LD'	0.68	0.040	0
κ_{\parallel}	43 ± 2.2 $\text{W m}^{-1} \text{K}^{-1}$	28 ± 1.2 $\text{W m}^{-1} \text{K}^{-1}$	14 ± 2.8 $\text{W m}^{-1} \text{K}^{-1}$
κ_{\perp}	0.085 ± 0.017 $\text{W m}^{-1} \text{K}^{-1}$

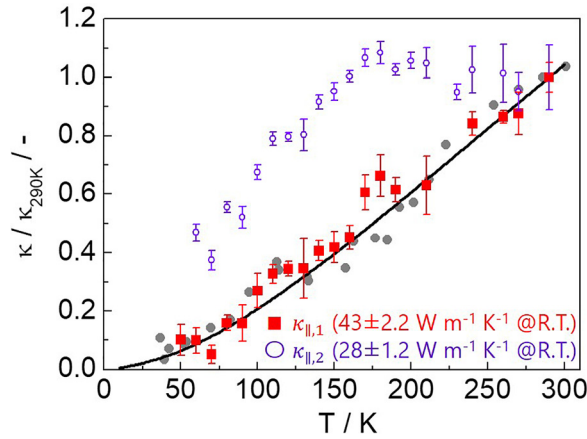


FIG. 2. Temperature dependence of thermal conductivity. ■: Film 1 (alignment direction), •: single CNT bundle,⁴³ ○: Film 2 (alignment direction), and solid line: simulated effective thermal conductivity of the highly aligned CNT film. The values of thermal conductivity are normalized by the RT value for each material.

the agreement in the temperature dependence between $\kappa_{||,1}$ and $\kappa_{||, \text{bundle}}$ suggests that the intertube thermal resistance has a limited effect on $\kappa_{||,1}$.

To further verify this suggestion, the internal thermal conductance of a CNT in the axial direction ($G_{||}$) and intertube thermal conductance at an aligned CNT-CNT contact (g) were calculated using the atomistic Green’s function (AGF) method.⁴⁵ The variables used for the models and calculations below are summarized in Table II. Note that since the CNT length is shorter than the average phonon mean free path,^{46–48} the phonon transport can be considered ballistic. As the average diameter (d) of consisting CNT of Film 1 is ~ 1.4 nm, a hexagonal unit cell consisting of (10,10) single-wall CNTs ($d = 1.36$ nm) was used as a representative atomic scale model for the calculations. While Film 1 contains both metallic and semiconducting

TABLE II. List of the variables used in the calculation and their details.

Variable	Explanation	Source
$G_{ }$	Internal thermal conductance of a CNT in the axial direction	AGF calculation
G_{\perp}	Internal thermal conductance of a CNT in the perpendicular direction	-
g	Intertube thermal conductance at an aligned CNT-CNT contact	AGF calculation
g_{exp}	Actual value of the intertube thermal conductance at R.T.	Model in Fig.4b
g'	Intertube thermal conductance at a CNT-CNT cross contact	Refs. 40 and 56
$\kappa_{ ,1,\text{eff}}$	The effective value of $\kappa_{ ,1}$	Model in Fig. 4(a)
$\kappa_{ ,2,\text{eff}}$	The effective value of $\kappa_{ ,2}$	Model in Fig. 4(c)
κ_{ind}	κ of each CNT constituting the Film 1	...
$\kappa_{ , \text{bundle}}$	κ of the CNT bundle	Ref. 43

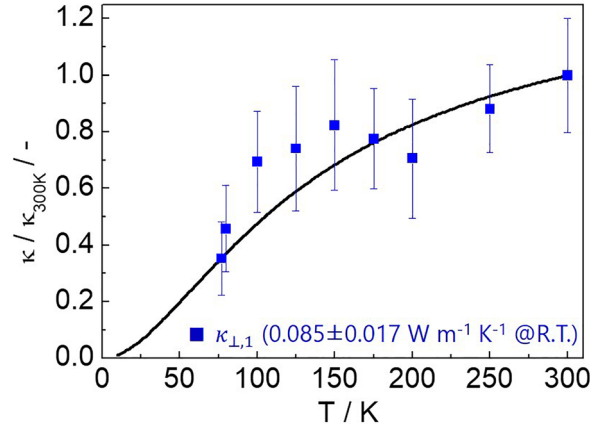


FIG. 3. ■: Normalized thermal conductivity of Film 1 in the perpendicular direction in the temperature range of 77–300 K and solid line: normalized simulated thermal conductance of highly aligned CNT in the perpendicular direction.

CNTs, the calculation result with metallic (10,10) CNTs is valid for comparison because heat transport in CNTs is dominated by phonons than by electrons.^{49,50} As shown in Figs. S2(a) and S2(b), the prepared cells for the alignment and perpendicular directions, respectively, were repeated twice in the section between the two leads. Periodic boundary conditions were applied in the directions of the cross section [Figs. S3(c) and S3(d)]. The interatomic interactions within and between CNTs were modeled by the Tersoff⁵¹ and Lennard-Jones potentials,⁵² respectively; the potential parameters are described in the references.

The effective value of $\kappa_{||,1}$ ($\kappa_{||,1,\text{eff}}$) was estimated by the following equation based on a model shown in Fig. 4(a):

$$\frac{L}{\kappa_{||,1,\text{eff}}} = \frac{1}{G_{||}} + \frac{1A}{gS}. \quad (1)$$

Here, L , A , and S represent the length, bottom area, and side area of a constituent CNT when CNTs are viewed as a honeycomb structure. The intertube term ($\frac{1A}{gS}$) includes the area ratio $\frac{A}{S}$ as $G_{||}$ and g both correspond to the thermal conductance per unit area, while the cross-sectional areas of heat conduction through CNTs and between CNTs are different. The temperature dependence of the calculated $\kappa_{||,1,\text{eff}}$ is plotted in Fig. 2, which agrees well with the experimental results. Here, the intertube term is around three orders of magnitude smaller than the internal term ($\frac{1}{G_{||}}$), indicating that the temperature dependence of $\kappa_{||,1,\text{eff}}$ reflects only that of internal thermal conductance. Therefore, from Eq. (1), $\kappa_{||,1,\text{eff}}$ can be approximated as

$$\kappa_{||,1,\text{eff}} = LG_{||}. \quad (2)$$

This equation can be further transformed to

$$\kappa_{||,1,\text{eff}} = A\kappa_{\text{ind}}, \quad (3)$$

where κ_{ind} represents κ of each CNT constituting the Film 1. This shows that, when phonon transport is ballistic (i.e., $G_{||}$ is constant), $\kappa_{||,1,\text{eff}}$ is determined only by the length of the constituent CNTs, or in other words, only by κ_{ind} . This explains the small observed $\kappa_{||,1}$ ($=43 \text{ W m}^{-1} \text{ K}^{-1}$); it is merely because the κ_{ind} values of constituent CNTs are small due to their shorter length (around 200 nm)

than those in the bundle in Ref. 43 (around 1 μm , giving $\kappa_{\parallel, \text{bundle}} = 200.2 \text{ W m}^{-1} \text{ K}^{-1}$), not because of the intertube thermal resistance. Note that it makes sense that the fivefold difference in the length results in the fivefold difference in κ as thermal conductivity increases linearly with the length when heat conduction is ballistic.⁵³

On the other hand, the intertube thermal resistance dominates the thermal conductivity of Film 1 in the cross-plane direction ($\kappa_{\perp, 1}$). This can be confirmed by good agreement in the temperature dependences of experimentally measured $\kappa_{\perp, 1}$ and calculated g (Fig. 3). Here, a quadratic increase at low temperatures and weak dependence at higher temperatures are observed, which is consistent with the temperature dependence of experimentally observed intertube thermal conductance between two CNTs.⁴⁴ Furthermore, the actual value of the intertube thermal conductance (g_{exp}) at RT was estimated from the experimental result ($\kappa_{\perp, 1}$) using a simple model shown in Fig. 4(b). In the calculation, the internal thermal conductance of a CNT in the perpendicular direction (G_{\perp}) was assumed to be much greater than g_{exp} . Based on the model, g_{exp} was calculated to be $1.5 \times 10^{-8} \text{ m}^2 \text{ K W}^{-1}$, which is close to g ($1.1 \times 10^{-8} \text{ m}^2 \text{ K W}^{-1}$) and the other reported values calculated by molecular dynamics (MD) simulations.^{54–56} This confirms that $\kappa_{\perp, 1}$ is mainly determined by the intertube thermal resistance.

It is also worth noting that the temperature dependence of $\kappa_{\parallel, 2}$ is different from that of $\kappa_{\parallel, 1}$ (Fig. 2). $\kappa_{\parallel, 2}$ increases sharply in the low temperature regime, while it becomes almost constant above 180 K. It is tempting here to discuss the result in terms of the peak temperature shift as the peak temperature of CNT materials is known to appear between 300 and 400 K, resulting from the competition between the increase in heat capacity and decrease in the phonon mean free paths due to Umklapp scattering with increasing temperature. However, as the constituent CNT material of Film 2 is exactly the same as that of Film 1, it is unlikely that their Umklapp scattering rates or the heat capacities significantly differ.

Instead, this temperature dependence of $\kappa_{\parallel, 2}$ can be explained by the stronger role of intertube thermal resistance at CNT-CNT cross contacts in Film 2 as shown in the simple model [Fig. 4(c)]. With this model, the effective κ_{\parallel} of Film 2 ($\kappa_{\parallel, 2, \text{eff}}$) can be estimated by the following equation:

$$\frac{L}{\kappa_{\parallel, 2, \text{eff}}} = \frac{1}{G_{\parallel}} + \frac{1}{g'}. \quad (4)$$

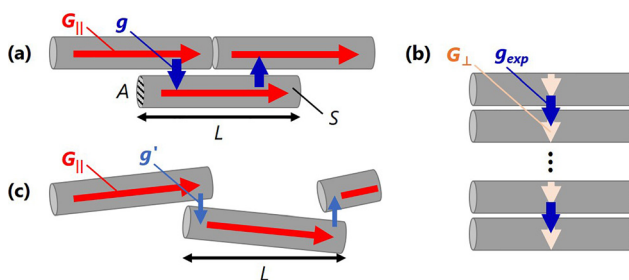


FIG. 4. (a) Simulation models to estimate the effective thermal conductivity of Film 1 in the alignment direction. L , A , and S represent the length, bottom area, and side area of constituent CNTs. G_{\parallel} represents the thermal conductance of internal CNT and g and g' represent the intertube thermal conductance at parallel/cross contact, respectively. (b) Simulation model for the calculation of intertube thermal resistance at CNT-CNT contact. (c) Simulation models to estimate the effective thermal conductivity of Film 2.

Here, g' represents the intertube thermal conductance at a CNT-CNT cross contact. Since the contact area is as small as the bottom area of CNT, the area ratio $\frac{A}{S}$ is not included in Eq. (4). According to the several reports clarifying the actual value of g' from simulations, it generally ranges from 10^8 to $10^9 \text{ W K}^{-1} \text{ m}^{-2}$,^{40,56} which is one to two orders of magnitude smaller than G_{\parallel} ($10^{10} \text{ W K}^{-1} \text{ m}^{-2}$ at RT). Therefore, in contrast to the case of $\kappa_{\parallel, 1, \text{eff}}$, the intertube term $\frac{1}{g'}$ is dominant in Eq. (4), and the temperature dependence of $\kappa_{\parallel, 2, \text{eff}}$ is expected to follow that of g' . The temperature dependence of g' has been investigated by both simulations⁵⁷ and experiments,⁴⁴ where g' showed a quadratic increase at low temperatures while the temperature dependence became very weak above 150 K, which is consistent with the behavior of $\kappa_{\parallel, 2}$ shown in Fig. 2. This indicates that the difference in temperature dependence between $\kappa_{\parallel, 1}$ and $\kappa_{\parallel, 2}$ arises from the difference in the leading mechanism of thermal resistance.

In conclusion, the κ of a highly aligned CNT film synthesized by the CVF method was measured in both the alignment direction and perpendicular direction. The κ value at RT was $43 \pm 2.2 \text{ W m}^{-1} \text{ K}^{-1}$ and $0.085 \pm 0.017 \text{ W m}^{-1} \text{ K}^{-1}$ in the alignment and perpendicular directions, respectively, yielding a thermal anisotropy of 500, the highest ever reported. Further analysis of the temperature dependence of κ_{\parallel} revealed that the effect of intertube thermal resistance, which is known to be large in previous CNT films with weaker alignment, has a negligible influence on the κ_{\parallel} owing to the large intertube contact area realized by the nearly perfect alignment, and κ_{\parallel} is determined only by κ of the constituent CNT length. This also suggests that the κ_{\parallel} can be even greater with longer constituent CNTs.

See the [supplementary material](#) for additional information regarding the synthesis method for CNT films, experimental setup, theoretical equation for the thermal measurement, details for the AGF calculation, and absolute values of experiment/simulation data.

This research was supported by JSPS KAKENHI Grant Number 19H00744. N.K., W.G., and J.K. acknowledge support from the Basic Energy Science (BES) program of the U.S. Department of Energy through Grant No. DE-FG02-06ER46308 (for preparation of aligned carbon nanotube films), the U.S. National Science Foundation through Grant No. ECCS-1708315 (for optical measurements), and the Robert A. Welch Foundation through Grant No. C-1509 (for structural characterization measurements). We thank M. Ouchi (Iwase Group, Waseda University) for providing technical support with the processing of measurement sample with the laser plotter and G. Timothy Noe II and Kevin Tian (Rice University) for proofreading this manuscript.

REFERENCES

- M. Fujii, X. Zhang, H. Xie, H. Ago, K. Takahashi, T. Ikuta, H. Abe, and T. Shimizu, *Phys. Rev. Lett.* **95**, 065502 (2005).
- E. Pop, D. Mann, Q. Wang, K. Goodson, and H. Dai, *Nano Lett.* **6**, 96 (2006).
- K. Yoshino, T. Kato, Y. Saito, J. Shitaba, T. Hanashima, K. Nagano, S. Chiashi, and Y. Homma, *ACS Omega* **3**, 4352 (2018).
- C. Yu, L. Shi, Z. Yao, D. Li, and A. Majumdar, *Nano Lett.* **5**, 1842 (2005).
- M. T. Pettes and L. Shi, *Adv. Funct. Mater.* **19**, 3918 (2009).
- M. B. Jakubinek, M. A. White, G. Li, C. Jayasinghe, W. Cho, M. J. Schulz, and V. Shanov, *Carbon* **48**, 3947 (2010).
- T. Tong, Y. Zhao, L. Delzeit, A. Kashani, M. Meyyappan, and A. Majumdar, *IEEE Trans. Compon. Packag. Technol.* **30**, 92 (2007).

- ⁸I. Ivanov, A. Puretzky, G. Eres, H. Wang, Z. Pan, H. Cui, R. Jin, J. Howe, and D. B. Geohegan, *Appl. Phys. Lett.* **89**, 223110 (2006).
- ⁹X. Wang, Z. Zhong, and J. Xu, *J. Appl. Phys.* **97**, 064302 (2005).
- ¹⁰L. Chen, B. Ju, Z. Feng, and Y. Zhao, *Smart Mater. Struct.* **27**, 075007 (2018).
- ¹¹X. J. Hu, A. A. Padilla, J. Xu, T. S. Fisher, and K. E. Goodson, *J. Heat Transfer* **128**, 1109 (2006).
- ¹²H. Xie, A. Cai, and X. Wang, *Phys. Lett. A* **369**, 120 (2007).
- ¹³D. J. Yang, Q. Zhang, G. Chen, S. F. Yoon, J. Ahn, S. G. Wang, Q. Zhou, Q. Wang, and J. Q. Li, *Phys. Rev. B* **66**, 165440 (2002).
- ¹⁴M. L. Bauer, Q. N. Pham, C. B. Saltonstall, and P. M. Norris, *Appl. Phys. Lett.* **105**, 151909 (2014).
- ¹⁵T. Borca-Tasciuc, S. Vafaei, D. A. Borca-Tasciuc, B. Q. Wei, R. Vajtai, and P. M. Ajayan, *J. Appl. Phys.* **98**, 054309 (2005).
- ¹⁶Z. L. Wang, Q. Li, and D. W. Tang, *Int. J. Thermophys.* **32**, 1013 (2011).
- ¹⁷L. Qiu, X. Wang, G. Su, D. Tang, X. Zheng, J. Zhu, Z. Wang, P. M. Norris, P. D. Bradford, and Y. Zhu, *Sci. Rep.* **6**, 21014 (2016).
- ¹⁸D. Wang, P. Song, C. Liu, W. Wu, and S. Fan, *Nanotechnology* **19**, 075609 (2008).
- ¹⁹A. E. Aliev, M. H. Lima, E. M. Silverman, and R. H. Baughman, *Nanotechnology* **21**, 035709 (2010).
- ²⁰Y. Inoue, Y. Suzuki, Y. Minami, J. Muramatsu, Y. Shimamura, K. Suzuki, A. Ghemes, M. Okada, S. Sakakibara, H. Mimura, and K. Naito, *Carbon* **49**, 2437 (2011).
- ²¹J. H. Pöhls, M. B. Johnson, M. A. White, R. Malik, B. Ruff, C. Jayasinghe, M. J. Schulz, and V. Shanov, *Carbon* **50**, 4175 (2012).
- ²²L. Zhang, G. Zhang, C. Liu, and S. Fan, *Nano Lett.* **12**, 4848 (2012).
- ²³T. S. Spann, S. M. Juckes, J. F. Niven, M. B. Johnson, J. A. Elliott, M. A. White, and A. H. Windle, *Carbon* **114**, 160 (2017).
- ²⁴J. E. Fischer, W. Zhou, J. Vavro, M. C. Llaguno, C. Guthy, R. Haggenmueller, M. J. Casavant, D. E. Walters, and R. E. Smalley, *J. Appl. Phys.* **93**, 2157 (2003).
- ²⁵P. Gonnet, Z. Liang, E. S. Choi, R. S. Kadambala, C. Zhang, J. S. Brooks, B. Wang, and L. Kramer, *Curr. Appl. Phys.* **6**, 119 (2006).
- ²⁶J. Hone, M. C. Llaguno, N. M. Nemes, A. T. Johnson, J. E. Fischer, D. A. Walters, M. J. Casavant, J. Schmidt, and R. E. Smalley, *Appl. Phys. Lett.* **77**, 666 (2000).
- ²⁷D. D. L. Chung and Y. Takizawa, *J. Electron. Mater.* **41**, 2580 (2012).
- ²⁸X. He, W. Gao, L. Xie, B. Li, Q. Zhang, S. Lei, J. M. Robinson, E. H. Hroz, S. K. Doorn, W. Wang, R. Vajtai, P. M. Ajayan, W. W. Adams, R. H. Hauge, and J. Kono, *Nat. Nanotechnol.* **11**, 633 (2016).
- ²⁹W. Gao and J. Kono, *R. Soc. Open Sci.* **6**, 181605 (2019).
- ³⁰C. Dames, S. Chen, C. T. Harris, J. Y. Huang, Z. F. Ren, M. S. Dresselhaus, and G. Chen, *Rev. Sci. Instrum.* **78**, 104903 (2007).
- ³¹A. J. Schmidt, X. Chen, and G. Chen, *Rev. Sci. Instrum.* **79**, 114902 (2008).
- ³²J. P. Feser and D. G. Cahill, *Rev. Sci. Instrum.* **83**, 104901 (2012).
- ³³T. Oyake, L. Feng, T. Shiga, M. Isogawa, Y. Nakamura, and J. Shiomi, *Phys. Rev. Lett.* **120**, 45901 (2018).
- ³⁴N. Komatsu, W. Gao, P. Chen, C. Guo, and A. Babakhani, *Adv. Funct. Mater.* **27**, 1606022 (2017).
- ³⁵K. Yanagi, R. Okada, Y. Ichinose, Y. Yomogida, F. Katsutani, W. Gao, and J. Kono, *Nat. Commun.* **9**, 1121 (2018).
- ³⁶W. Gao, X. Li, M. Bamba, and J. Kono, *Nat. Photonics* **12**, 362 (2018).
- ³⁷K. Fukuhara, Y. Ichinose, H. Nishidome, Y. Yomogida, F. Katsutani, N. Komatsu, W. Gao, J. Kono, and K. Yanagi, *Appl. Phys. Lett.* **113**, 243105 (2018).
- ³⁸F. Katsutani, W. Gao, X. Li, Y. Ichinose, Y. Yomogida, K. Yanagi, and J. Kono, *Phys. Rev. B* **99**, 035426 (2019).
- ³⁹W. Gao, C. Doiron, X. Li, J. Kono, and G. V. Naik, *ACS Photonics* **6**, 1602 (2019).
- ⁴⁰R. S. Prasher, X. J. Hu, Y. Chalopin, N. Mingo, K. Lofgreen, S. Volz, F. Cleri, and P. Keblinski, *Phys. Rev. Lett.* **102**, 105901 (2009).
- ⁴¹L. Shi, D. Li, C. Yu, W. Jang, D. Kim, Z. Yao, P. Kim, and A. Majumdar, *J. Heat Transfer* **125**, 881 (2003).
- ⁴²I. K. Hsu, M. T. Pettes, A. Bushmaker, M. Aykol, L. Shi, and S. B. Cronin, *Nano Lett.* **9**, 590 (2009).
- ⁴³T. Kodama, M. Ohnishi, W. Park, T. Shiga, J. Park, T. Shimada, H. Shinohara, J. Shiomi, and K. E. Goodson, *Nat. Mater.* **16**, 892 (2017).
- ⁴⁴J. Yang, S. Waltermire, Y. Chen, A. A. Zinn, T. T. Xu, and D. Li, *Appl. Phys. Lett.* **96**, 023109 (2010).
- ⁴⁵T. Markussen, A. P. Jauho, and M. Brandbyge, *Phys. Rev. B* **79**, 035415 (2009).
- ⁴⁶K. Sääskilähti, J. Oksanen, S. Volz, and J. Tulkki, *Phys. Rev. B* **91**, 115426 (2015).
- ⁴⁷S. P. Hepplestone and G. P. Srivastava, *J. Phys.: Conf. Ser.* **92**, 012076 (2007).
- ⁴⁸P. Kim, L. Shi, A. Majumdar, and P. L. McEuen, *Phys. Rev. Lett.* **87**, 215502 (2001).
- ⁴⁹A. A. Balandin, *Nat. Mater.* **10**, 569 (2011).
- ⁵⁰A. M. Marconnet, M. A. Panzer, and K. E. Goodson, *Rev. Mod. Phys.* **85**, 1295 (2013).
- ⁵¹L. Lindsay and D. A. Broido, *Phys. Rev. B* **81**, 205441 (2010).
- ⁵²O. N. Kalugin, V. V. Chaban, and O. V. Prezhdo, *Carbon Nanotubes—Synthesis, Characterization, Applications* (IntechOpen, 2011), p. 325.
- ⁵³N. Mingo and D. A. Broido, *Nano Lett.* **5**, 1221 (2005).
- ⁵⁴A. N. Volkov, R. N. Salaway, and L. V. Zhigilei, *J. Appl. Phys.* **114**, 104301 (2013).
- ⁵⁵H. Zhong and J. R. Lukes, *Phys. Rev. B* **74**, 125403 (2006).
- ⁵⁶W. J. Evans, M. Shen, and P. Keblinski, *Appl. Phys. Lett.* **100**, 261908 (2012).
- ⁵⁷Y. Chalopin, S. Volz, and N. Mingo, *J. Appl. Phys.* **105**, 084301 (2009).